Indian J. Met. Hydrol. Geophys. (1976), 27, 4, 409—416

551.511.3 : 551.515.31 (54)

Computation of divergence and vorticity from observed winds over the Indian region during monsoon

Y. RAMANATHAN and M. R. BASSI

Meteorological Office, New Delhi

(*Received 15 March 1975*)

ABSTRACT. Grid-point wind data at 1000, 850, 700, 500, 300 and 200 mb derived from station observations by manual analysis are subjected to finite Double Fourier analysis, to compute analytically the vorticity and divergence values from the amplitudes of the Fourier components. These are compared with the values obtained by the conventional central difference method. The truncation errors are found to be less than 30 per cent in 95 per cent of the cases. The vorticity values are generally $\sim 10^{-5}$ sec^{-1} and are about twice that of divergence values. For vorticity values exceeding $\sim 5 \times 10^{-5}$ sec^{-1} in the depression region, the divergence is found to be one order less. For low values of vorticity, *i.e.*, less than $\sim 5 \times 10^{-5}$ sec^{-1} the divergence is of the same order.

1. Introduction

Computation of divergence and vorticity are generally made by the method of finite differences using a central difference scheme, limiting the Tailor series expansion for the differential coefficients to three terms. The truncation errors involved are usually assumed to be negligible. For these computations it is also considered more appropriate to use the wind field in the tropics, where the prsesure field adjust to the wind field. (Houghton and Washington 1969). However, use of observed winds for determining the divergence at least, is beset with difficulties. The magnitude of the error in the observed winds is considered to be only one order less than that of the winds themselves. Hence the error in computing the large-scale divergence and vorticity, it is argued, should be of the same order as the divergence and vorticity values themselves. Charney (1948) showed from scale analysis of atmospheric motions in the middle latitudes that the two terms $\partial u/\partial x$ and $\partial v/\partial y$ comprising the the horizontal divergence are of opposit sign and of the same order $\sim 10^{-5}$ sec^{-1}. On the other hand, in the computation of vorticity, the errors in the two terms $\partial v/\partial x$ and $\partial u/\partial y$ perhaps cancel each other on subtraction, or one of the two terms is one order higher than the other, and more reliable estimates of vorticity are obtained. Despite these difficulties, observed winds have been used for the divergence and vorticity computations over the Indian region by several authors (Das 1951, Dutta and Baghare 1968 and Sajnani 1968) applying smoothing processes to eliminate the small-scale noise. The magnitude of the vorticity and divergence values were found by these authors to be of the same order $\sim 10^{-5}$sec^{-1}. Fleagle (1946) also computed divergences of $\sim 10^{-5}$ sec^{-1} from actual wind observations. On the other hand, magnitudes of $\sim 10^{-6}$ sec^{-1} were obtained by Namias and Clapp (1946) using 5-day mean charts. In this case, the small-scale noise of large divergences appear to have been more effectively eliminated by the computation of the means.

The motivations for the present study are —(*i*) to estimate the order of magnitudes of divergence and vorticity after eliminating the small-scale noise effectively and (*ii*) to examine the feasibility of using the finite difference method for the computations from an estimation of the truncation errors involved. Towards this end, the grid-point data were first analysed by the method of Double-Fourier technique. From the Fourier amplitudes the divergence and vorticity were computed and compared with those by the finite-difference method from the analysed data. Accordingly, Section 2 describes the method of computation. Description of the data and diagrams are found in the Section 3. A discussion of the results follows in the fourth section.

2. List of Symbols

- X Distance (km) along the zonal direction
- Y Distance (km) along the meridional direction
- L Length (km) of the domain
- D Breadth (km) of the domain
- k Fundamental wave number along X
- l Fundamental wave number along Y

m	Harmonic of k
n	Harmonic of l
M	Total harmonics m
N	Total harmonics n
u	Zonal wind component (m/sec)
v	Meridonal wind component (m/sec)
I	Grid-point count along X
J	Grid-point count along Y
X_I	X distance (km) of the I^{th} point
Y_J	Y distance (km) of the J^{th} point
$U_{(m,n)}$	amplitude (m/sec) of the harmonic (m, n) for u field
$V_{(m,n)}$	Same as above for v field
$A_{(m,n)}$	Same as above for any scalar S
A_R, A_I	Real and imaginary parts of A
ADIV, AVORT	Divergence and vorticity (sec^{-1}) computed from Fourier amplitudes
DIV, VORT	Same as above from Finite-differences
DERR, VERR	Percentage relative error in divergence and vorticity for computation by finite-difference method
ORDER	Divergence/Vorticity
I_{max}	Total number of grid-points along X
J_{max}	Total number of grid-points along Y

3. Method of computation

From the data of wind direction and speed at the grid points in the chosen domain, scalar u and v components were first computed. Each of these scaler fields were then subjected to a finite double Fourier analysis (details in the Appendix I). Thirty-one Fourier components were found adequate to describe all the features of the charts, with the root mean square error between the actual and fitted data as low as 1 m/sec. By this the small-scale noise in the data were sought to be eliminated. The actual data were now discarded and all the computations for the finite-difference method also were made from the fitted data only.

Using the amplitudes of the Fourier components, the divergence and vorticity at each of the grid-points (I, J) were now computed.

If

$$u_{I,J} = \sum_{m=-M}^{M} \sum_{n=-N}^{N} U_{(m,n)} e^{-i(mkx_I + nly_J)} \tag{2·1}$$

and

$$v_{I,J} = \sum_{m=-M}^{M} \sum_{n=-N}^{N} V_{(m,n)} e^{-i(mkx_I + nly_J)} \tag{2·2}$$

the divergence and vorticity values could be determined analytically from

$$\text{ADIV}_{(I,J)} = \left(\frac{\partial u}{\partial x}\right)_{I,J} + \left(\frac{\partial v}{\partial y}\right)_{I,J} \tag{2.3}$$

$$\text{AVORT}_{(I,J)} = \left(\frac{\partial v}{\partial x}\right)_{I,J} - \left(\frac{\partial u}{\partial y}\right)_{I,J} \tag{2·4}$$

Where,

$$\left(\frac{\partial u}{\partial x}\right)_{I,J} = -i \sum\sum U_{(m,n)} mk e^{-i(mkx_I + nly_J)} \tag{2·5}$$

$$\left(\frac{\partial v}{\partial y}\right)_{I,J} = -i \sum\sum V_{(m,n)} nl e^{-i(mkx_I + nly_J)} \tag{2·6}$$

$$\left(\frac{\partial v}{\partial x}\right)_{I,J} = -i \sum\sum V_{(m,n)} mk e^{-i(mkx_I + nly_J)} \tag{2·7}$$

and

$$\left(\frac{\partial u}{\partial y}\right)_{I,J} = -i \sum\sum U_{(m,n)} nl e^{-i(mkx_I + nly_J)} \tag{2·8}$$

From the central-difference scheme, at a grid point (I,J)

$$\text{DIV}_{(I,J)} = \frac{u_{I+1,J} - u_{I-1,J}}{2 \triangle x} + \frac{v_{I,J+1} - V_{I,J-1}}{2 \triangle y} \tag{2.9}$$

$$\text{VORT}_{(I,J)} = \frac{v_{I+1,J} - v_{I-1,J}}{2 \triangle x} - \frac{u_{I,J+1} - u_{I,J-1}}{2 \triangle y} \tag{2.10}$$

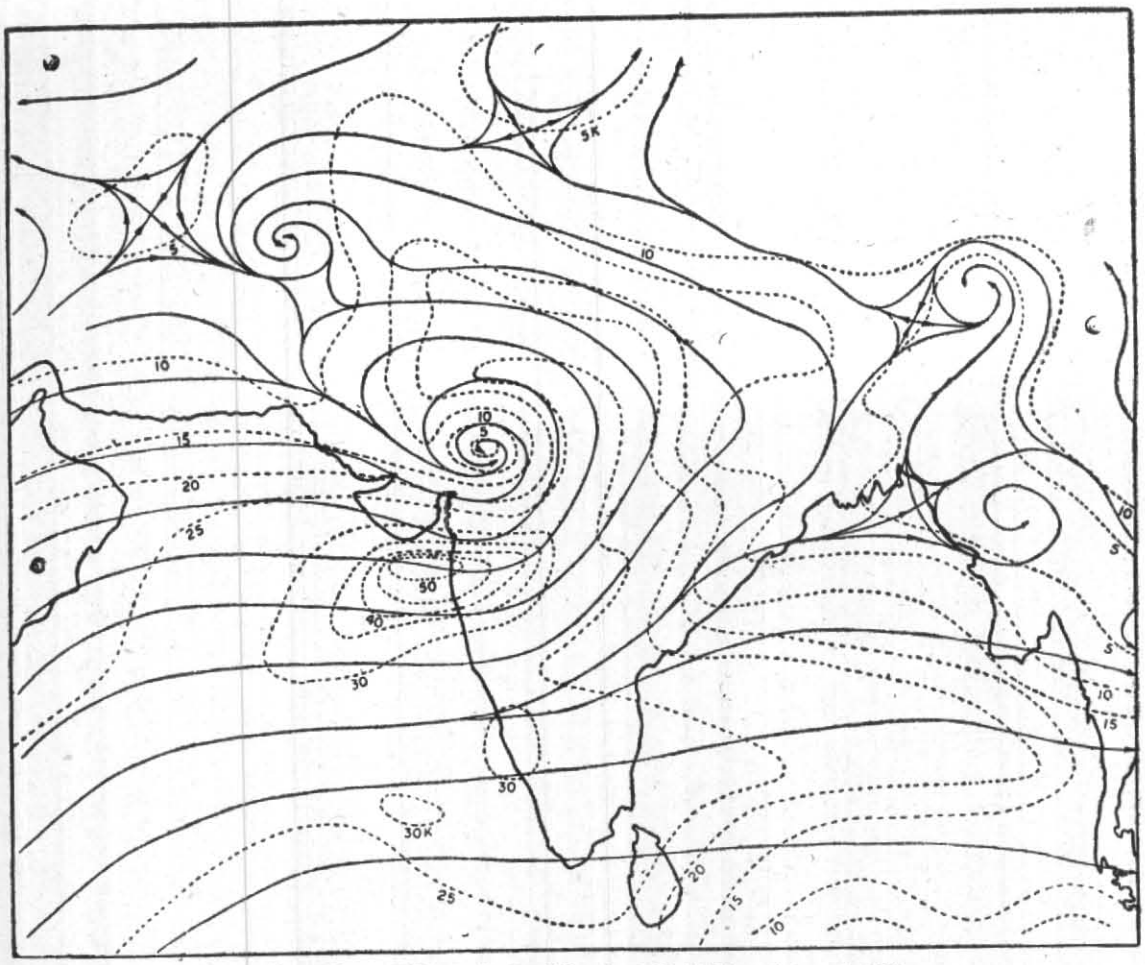

Fig. 1. Streamlines and isotachs for 850 mb at 00 GMT on 6 August 1968

The curvature terms in both the expressions were neglected. The percentage relative error at the grid point (I,J)

$$\text{DERR}_{(I,J)} = \frac{\text{ADIV}_{(I,J)} - \text{DIV}_{(I,J)}}{\text{ADIV}_{(I,J)}} \times 100 \qquad (2{\cdot}11)$$

$$\text{VERR}_{(I,J)} = \frac{\text{AVORT}_{(I,J)} - \text{VORT}_{(I,J)}}{\text{AVORT}_{(I,J)}} \times 100 \qquad (2{\cdot}12)$$

would give an estimate of the truncation error in the divergence and vorticity computations by the finite-difference method, respectively.

The order of the relative magnitudes of divergence and vorticity at each grid-point could be estimated from

$$\text{ORDER}_{(I,J)} = \frac{\text{ADIV}_{(I,J)}}{\text{AVORT}_{(I,J)}} \qquad (2{\cdot}13)$$

Only the absolute values of ADIV and AVORT were taken for this computation.

4. Data and Diagrams

The computations were made for a number of monsoon situations, and a case study typical of them is presented in this section. The situation was that of 6 August 1968 at 00 GMT for the area Lat 6°N to 36°N and Long. 56°E to 108°E, with a monsoon depression located at 24·0°N and 74°E over land extending up to 500 mb. Grid point data of wind direction and speed at 1000, 850, 700 500, 300 and 200 mb were picked from manual analysis at an interval of 2° Lat./Long. Fig. 1 gives the 850 mb streamlines and isotachs. Fig. 2 gives the vorticity and divergence profiles in the cross-section along 74°E through the depression. The component distributions of $\partial u/\partial x$, $\partial v/\partial y$, $\partial v/\partial x$ and $\partial u/\partial y$ are also shown. All these computations are from Fourier amplitudes. In Fig. 3 cumulative frequency diagrams for the order of divergence/vorticity are presented. These are the ogives or the cumulative frequency distribution curves as the

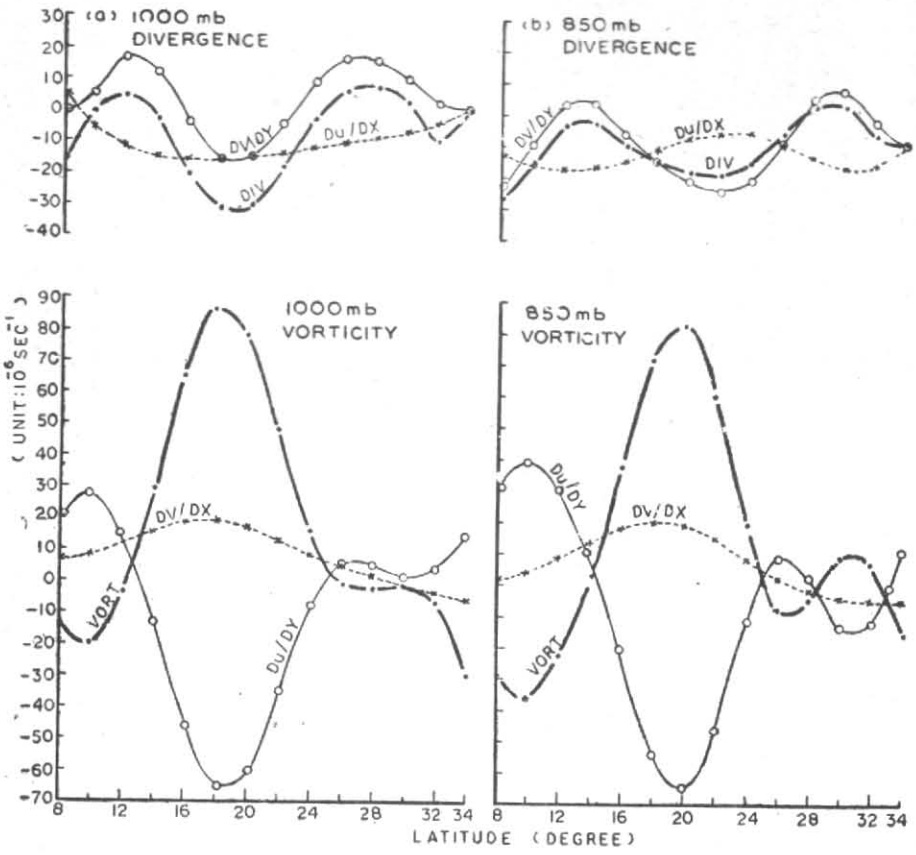

Fig. 2 *a* and (*b*)

Divergence & vorticity profile at (*a*) 1000 mb and (*b*) 850 mb levels in the cross-section along 74°E with component distribution $\partial u/\partial x$, $\partial v/\partial y$, $\partial v/\partial x$ and $\partial u/\partial y$.

percentage of the total observations. The abscissa gives the central values of the class-intervals. By reading an ordinate value against a particular class interval, it is possible to know as to what percentage of observations lies below a particular class-interval. A few values of order greater than 1 found in the case of vorticity values $\sim 10^{-6}$ sec^{-1} were also included in the class-interval centred 1. The curves for vorticity values $\sim 10^{-5}$ sec^{-1} (above $0{\cdot}5 \times 10^{-5}$ sec^{-1}) and for values $\sim 10^{-6}$ sec^{-1} (below $0{\cdot}5 \times 10^{-5}$) are shown separately. Fig. 4 shows cumulative frequency diagrams for the percentage truncation errors. The urves for vorticity and divergence are separately shown.

5. Discussion

Considering the field as a whole including the computations at all levels, about 65% of the values had vorticity values $\sim 10^{-5}$ sec^{-1} and greater and about 35% values were $\sim 10^{-6}$ sec^{-1} and less. It was just the reverse in the case of divergence, *viz.*, 65% of the values were $\sim 10^{-6}$ sec^{-1} and 35% of the values were $\sim 10^{-5}$ sec^{-1} Level by level also, these proportions were the same to a variation of 2 to 3%. From the gives in Fig. 3, it could be seen that 65%-70% of the values were at least twice that of the divergence values for the normal vorticity values $\sim 10^{-5}$ scc^{-1} (65% of the total). For the vorticity value $\sim 10^{-6}$ sec^{-1} (35% of the total), the divergence values were of the same order as the vorticity values. This was the same for all the levels. From Fig. 2 it could be seen that the vorticity values were very large in the region of the depression at all levels up to 500 mb. A typical value was 8×10^{-5} sec^{-1}. The level of 300 mb was perhaps nearer the transition level from the westerlies to

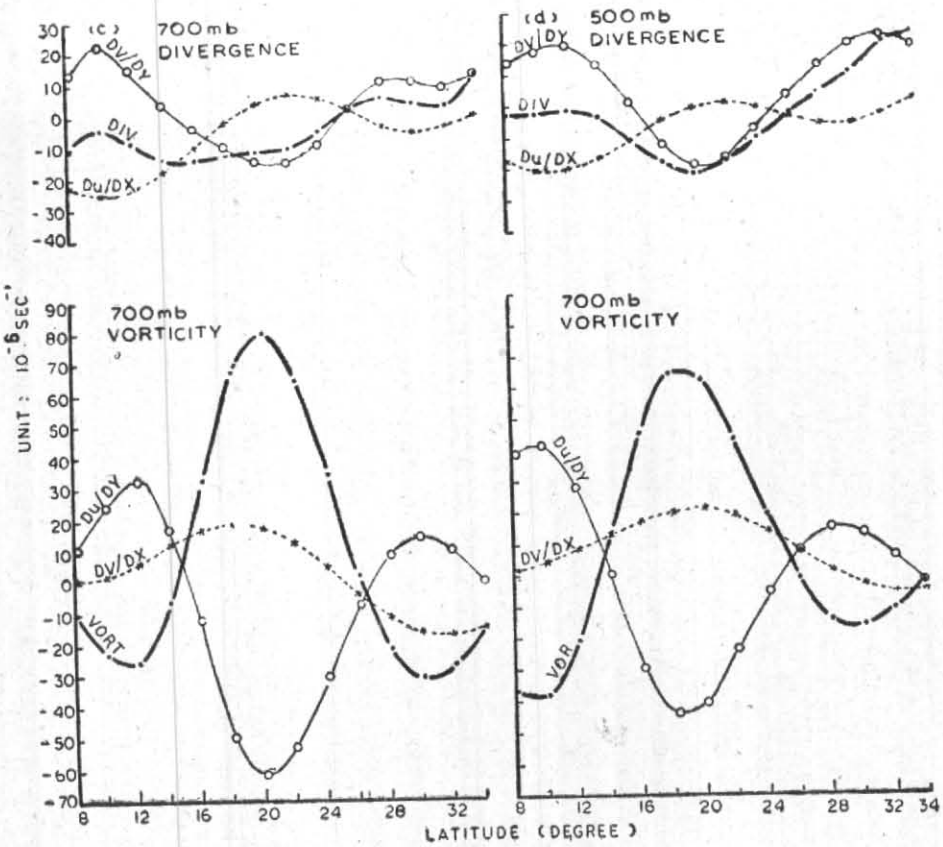

Fig. 2 (c and d). Divergence and vorticity profile at(c) 700 mb and (d) 500 mb levels

the easterlies and the vorticity values were much smaller and were of the same order as the divergence values. It was also noticed that the divergence values in the region of the depression were definitely one order less than the vorticity values. This was the same as in middle latitudes. Another interesting feature was the dominance of the meridional veriation terms $\partial v/\partial y$ and $\partial u/\partial y$ in the divergence and vorticity computations, whenever the vorticity and divergence values were high. This was also noticed in the region of the depression (Fig. 2). Fig. 4 presents a very encouraging picture for the computation of vorticity and divergence by the central finite-difference method. In general, more than 60% of the computations showed a truncation error of 10% or less, and more than 95% of the values showed an error of 30% and less. It was also seen that the smaller values showed greater truncation errors. Since the smaller divergence and vorticity values even with more than 30% error in truncation have small absolute errors: this may perhaps not be serious. Though it may not be practicable to adopt the technique of finite Fourier analysis to eliminate the small-scale noise in each case still it is possible to derive meaningful estimates of divergence and vorticity by finite difference methods, after carefully analysing and smoothing the data to minimise small-scale noise of spurious divergence. The grid distance must also be as small as practicable to minimise truncation errors.

6. Conclusion

From the study it was seen that the vorticity values were :

(*i*) One order more than the divergence values in the region of depressions.

(*ii*) At least twice that of divergence normally when the vorticity values were $\sim 10^{-5}$ sec^{-1}.

(*iii*) Of the same order as divergence when the vorticity values were $\sim 10^{-6}$ sec^{-1}.

(*iv*) The meridional variational terms were more dominant than the zonal variation terms generally and especially in the region of the monsoon depression.

(*v*) Since the truncation errors were found to be less than 30% in 95% of the computations, the central finite-difference scheme could give reliable estimate

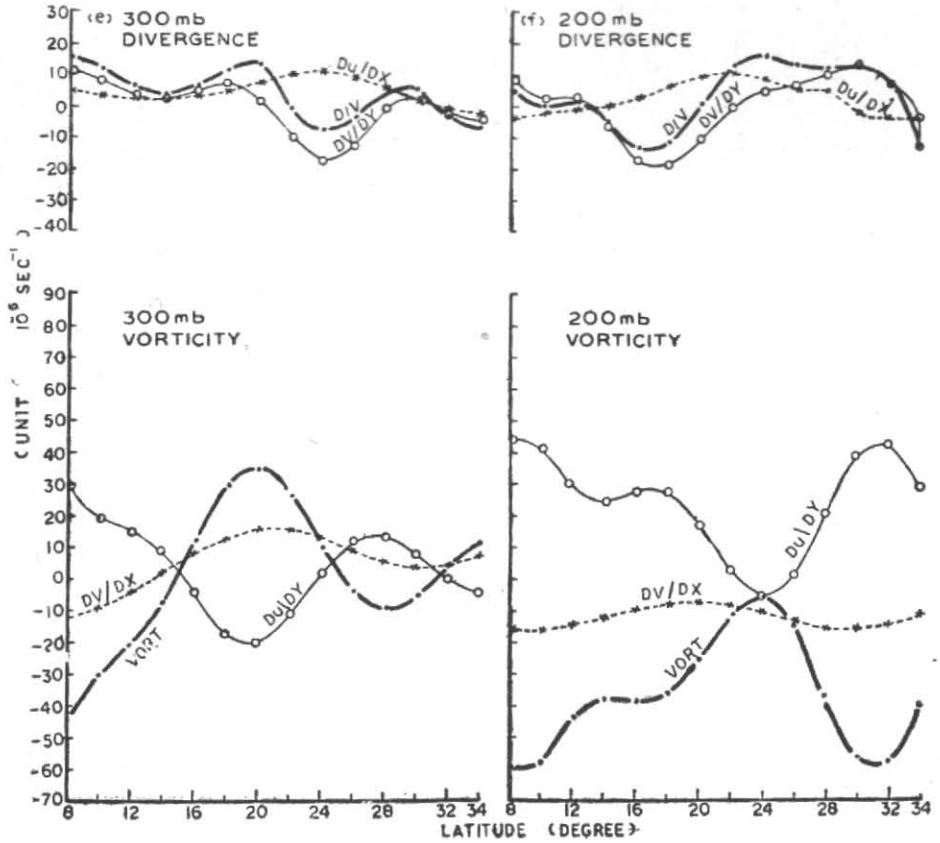

Fig. 2 (e and f) Divergence and vorticity profile at (e) 300 mb and (f) 200 mb levels

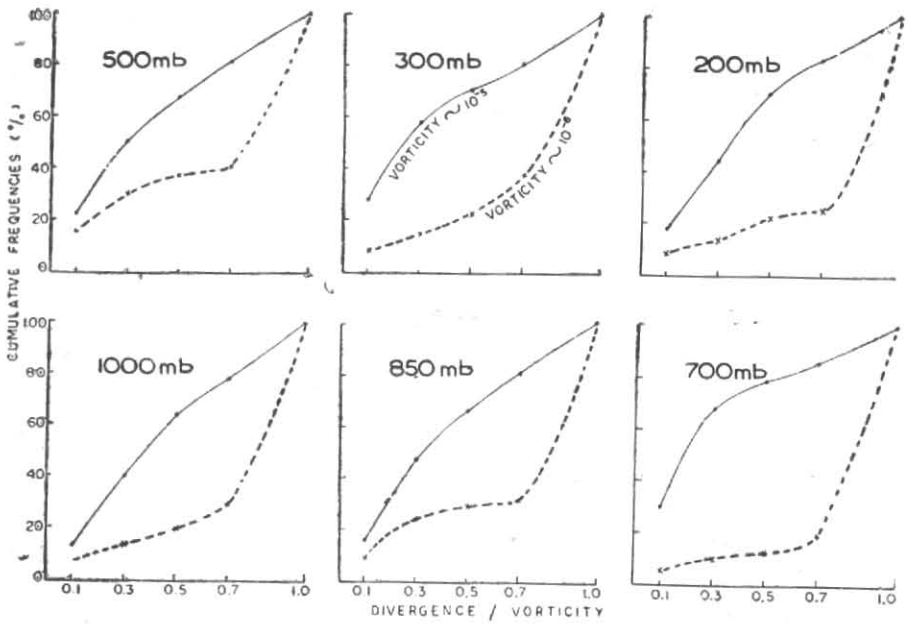

Fig. 3. Cumulative frequency diagram for the order of divergence/vorticity values

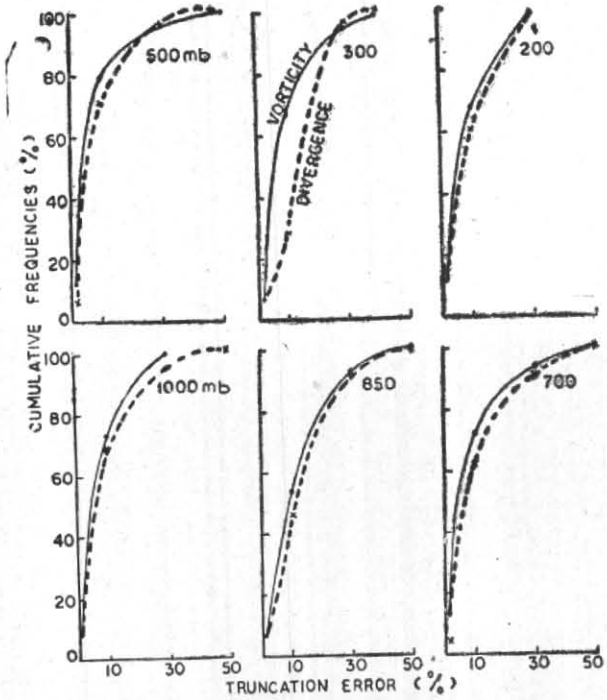

Fig. 4. Cumulative frequency diagram for truncation errors

of vorticity and divergence, provided the data are smoothed and grid interval chosen as small as practicable.

Acknowledgements

The authors thank Dr. P. S. Pant for his encouragement and interest in the study. They also express their sincere thanks to Shri D. R. Sikka for making available to them the grid-point data which he used for some other studies. They also convey their thanks to Shri Hari Kishan for preparing the diagrams and to Miss S. L. Thapar for typing the manuscript.

REFERENCES

Charney, J. G. 1948 On the scale of Atmospheric motions.

Das, P. K. 1951 a *Geophys., Publikasjoner*, **17**, No. 2, 17 pp.

1951 b *Indian J. Met. Geophys.*, 2, 3,pp. 172-179.

Dutta, R. K., and Baghare, M. M. 1968 Prognostication of divergence field in Tropics. Proc. Symp. Num. Weath. Pred., Tokyo, III-97-III-102.

Fleagle, R. G. 1946 *J. Met.*, **3**, 9-13.

Houghton, D. and Washington, W. 1969 *J. Appl. Met.*, **8**, 726-737.

Namias, J. and Clapp., P.F. 1969 *Ibid.*, **3**, 14-22.

Sajnani, P. P. 1968 Use of observed winds for computation of divergence and vorticity over India. Proc. Symp. Num. Weath. Pred. Tokyo, VI-45-VI-52.

APPENDIX I

Double Fourier Analysis Technique

Let $S_{(I, J)}$ be the grid-point value of any scalar S.

$$F_{(I, J)} = \sum_{m=-M}^{M} \sum_{n=-N}^{N} A_{(m, n)} \exp\left[-i\,(mkx_I + nly_J)\right] \tag{A.1}$$

is the scalar value at the grid-point (I, J) from the total contribution of the included harmonics, for the least-square fit we have

$$\sum_{I=1}^{I_{max}} \sum_{J=1}^{J_{max}} [S_{(I, J)} - F_{(I, J)}]^2 \text{ is a minimum} \tag{A.2}$$

i. e.,

$$\sum_{I=1}^{I_{max}} \sum_{J=1}^{J_{max}} \left[S_{(I, J)} - \sum_{m=-M}^{M} \sum_{n=-N}^{N} \{A_{(m, n)} \exp - i\,(mkx_I + nly_J\} \right]^2$$

is a minimum (A. 3)

Since $S_{(I, J)}$ is real, we consider only the real part of $A_{(m, n)}$ *i.e.*,
$A_R\,(m, n) \cos\,(mkx_I + nly_J) + A_I\,(m, n) \sin\,(mkx_I + nly_J)$

The normal equation of (A.2) written in matrix form

$$\begin{vmatrix} 1 & \Sigma\Sigma \cos kx_I & \Sigma\Sigma \cos\,(kx_I + ly_J) & \ldots\ldots \Sigma\Sigma \sin kx_I & \ldots \\ \Sigma\Sigma \cos kx_I & \Sigma\Sigma\,(\cos kx_I)^2 & \Sigma\Sigma \cos kx_I \cos\,(kx_I + ly_J) & \ldots\ldots \Sigma\Sigma \cos kx_I \sin kx_I & \ldots \\ \Sigma\Sigma \sin kx_I & . & . & \ldots \Sigma\Sigma\,(\sin kx_I)^2 & \ldots \\ \ldots & & \ldots & & \ldots \end{vmatrix} \begin{vmatrix} A_R\,(_{0,0}) \\ A_R\,(_{1,0}) \\ A_I\,(_{0,1}) \\ \end{vmatrix} = \begin{vmatrix} \Sigma\Sigma \text{ SIJ} \\ \Sigma\Sigma \text{ SIJ} \cos kx_I \\ \Sigma\Sigma \text{ SIJ} \sin kx_I \end{vmatrix} \tag{A.4}$$

Solving the matrix equation (A. 4) we get A_Rs and A_Is and inserting them in equation (A.1) we get $F_{(I,J)}$ at the grid-points. By experience it was found that in finite Fourier analysis inclusion of negative harmonics in either X or Y direction was adequate for proper representation of the flow features.

The 31 included harmonics in the present case were :

m	0	1	0	2	1	1	0	3	2	2	1	1	0	4	3	3	2	2	1	1	0	5	4	4	3	3	2	2	1	1	0
n	0	0	1	0	1	-1	2	0	1	-1	2	-2	3	0	1	-1	2	-2	3	-3	4	0	1	-1	2	-2	3	-3	4	-4	5